NANO LETTERS

Letter

pubs.acs.org/NanoLett

Single Cell GFP-Trap Reveals Stoichiometry and Dynamics of Cytosolic Protein Complexes

Tim Wedeking, Sara Löchte, Christian P. Richter, Maniraj Bhagawati, Jacob Piehler,* and Changjiang You*

Department of Biology, University of Osnabrück, 49076 Osnabrück, Germany

Supporting Information

ABSTRACT: We developed in situ single cell pull-down (SiCPull) of GFP-tagged protein complexes based on micropatterned functionalized surface architectures. Cells cultured on these supports are lysed by mild detergents and protein complexes captured to the surface are probed in situ by total internal reflection fluorescence microscopy. Using SiCPull, we quantitatively mapped the lifetimes of various signal transducer and activator of transcription complexes by monitoring dissociation from the surface and defined their stoichiometry on the single molecule level.

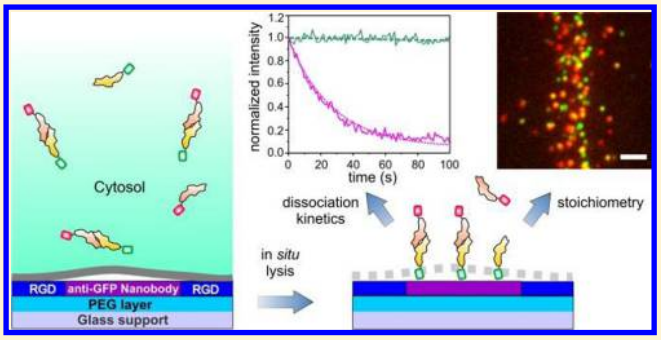

KEYWORDS: *Protein−protein interaction, functional surface micropatterning, nanobody, signal transducer and activator of transcription, single molecule imaging*

Dynamic protein−protein interactions of cytosolic protein complexes play a key role in regulating propagation of cellular signaling.[1,2] While new spectroscopic methods for detecting protein interactions in living cells are currently emerging,[3,4] reliable characterization of binding affinities, interaction kinetics, and the stoichiometry of complexes still requires their isolation from cell lysates. The standard methods for identification of interaction partners are coimmunoprecipitation (co-IP) and pull-down assays in combination with Western blotting or mass spectrometry.[5−7] These methods are based on copurifying interaction partners (prey) using affinity chromatography of a bait protein. Thus, the composition of complexes can be reliably identified, while the stoichiometry and the dynamics of complexes cannot be quantified by these methods. Moreover, transient protein complexes (K_D > 1 μM) are difficult to be reliably probed by these techniques as prey proteins rapidly dissociate and are therefore lost during washing steps. To overcome these limitations, single-molecule pull-down (SiMPull)[8−11] and single molecule co-IP (SiCoIP)[12,13] have recently been pioneered. Using antibody-functionalized surfaces, protein complexes were captured directly from cell lysates for in situ analysis by single molecule imaging techniques.[8,12] Under these conditions, reliable determination of the stoichiometry of transient protein complexes down to subsecond lifetimes has been successfully demonstrated.[13]

Exploiting the concept that only few molecules are required for SiMPull, we have here further advanced this approach by engineering surface architectures suitable for pull-down assays directly from individual mammalian cells grown on the surface of a microscopy cover slide. For ensuring highly specific and efficient surface capturing and for providing internal referencing, we have developed binary surface micropatterning methods based on a poly(ethylene glycol) (PEG) polymer brush, which was functionalized with a high-affinity anti-GFP nanobody[14] (NB) (Figure 1a). Upon cell lysis, for example, by means of a mild detergent, GFP-tagged bait proteins released from the cytosol are specifically captured into micropatterns by the NB and interacting prey proteins are concomitantly monitored by total internal reflection fluorescence (TIRF) microscopy (Figure 1b). As the protein concentration and thus the surface capturing probability decays very rapidly with the distance from the position of each cell ($\sim r^{-3}$), protein complexes can be analyzed immediately after their release from the cytosol on the single cell level.

For efficient cell growth on the strongly protein-repelling, PEGylated substrate, RGD peptides were presented in orthogonal micropatterns (Figure 1a), thus providing spatially separated areas for cell attachment via focal adhesion and for the pull-down of cellular proteins. Micropatterned surface functionalization moreover provides distinct signal-to-background contrast as internal controls for reliably identifying pulldown specificity.[15] Initial attempts for capturing EGFP expressed in HeLa cells, which were grown on coverslides homogeneously functionalized with NB and RGD (Supporting Information Figure S1) corroborated the necessity for internal referencing by surface micropatterning. For binary micropatterning of NB and RGD, robust and versatile photolithography and microcontact printing-based strategies were

Received: March 24, 2015
Revised: April 20, 2015
Published: April 22, 2015

DOI: 10.1021/acs.nanolett.5b01153
Nano Lett. 2015, 15, 3610−3615

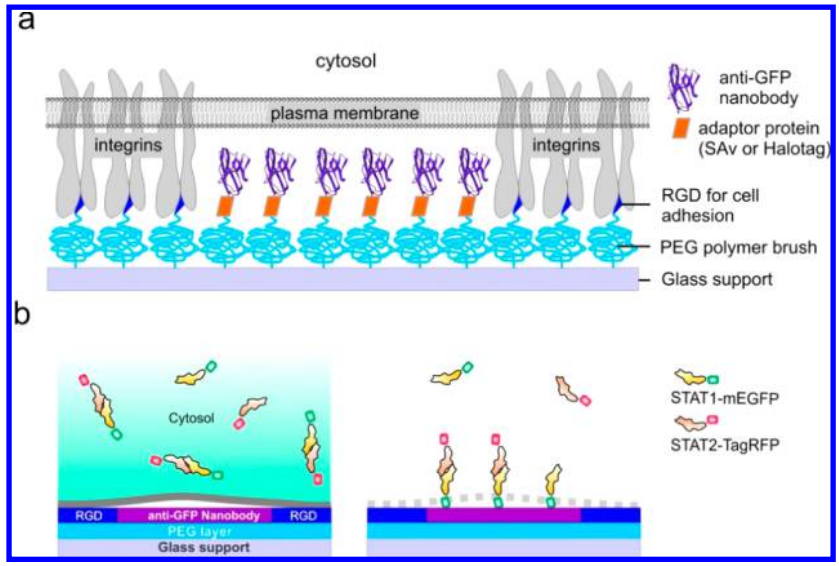

Figure 1. Single cell pull-down (SiCPull) of cytosolic protein complexes. (a) Surface architecture for SiCPull assays comprising binary micropatterns of RGD peptide and NB (see also Supporting Information Figure S2) for cell adhesion and bait capturing, respectively. (b) The concept of SiCPull: cells are cultivated on the binary functionalized surface with the bait (e.g., STAT1-mEGFP) and prey (e.g., STAT2-TagRFP) proteins expressed in the cytosol (left). The plasma membrane is disintegrated by mild detergent to release the cytosolic proteins for in situ pull-down (right).

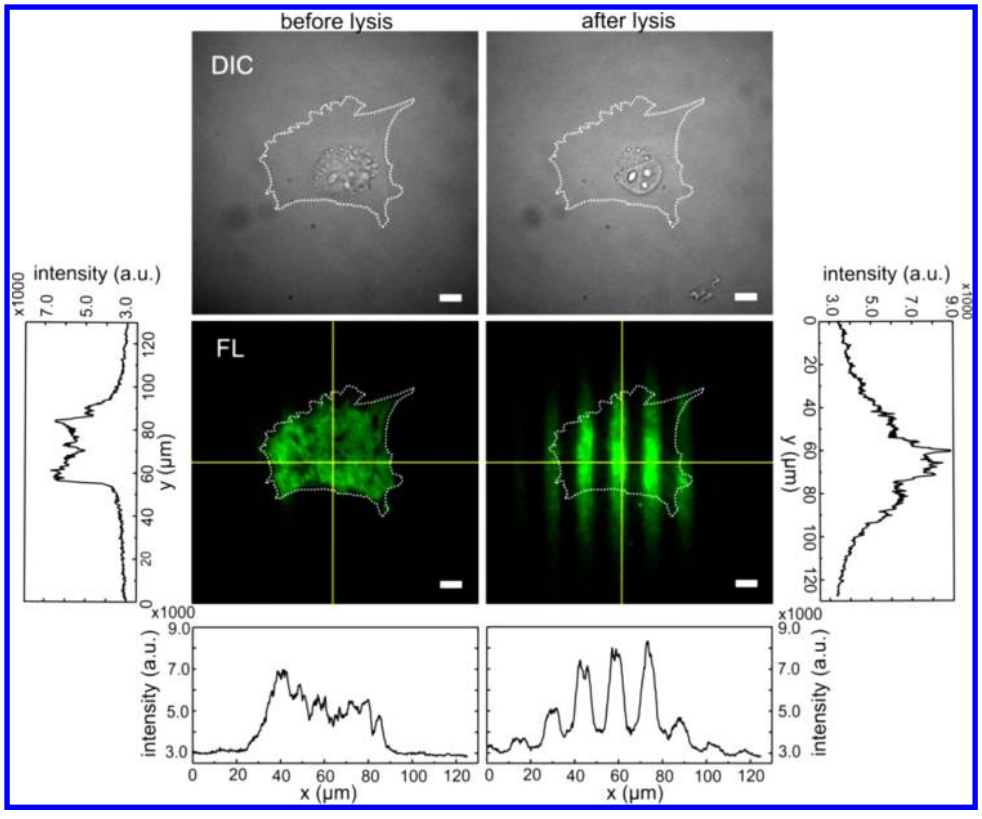

Figure 2. Capturing of STAT1-mEGFP from a single HeLa cell visualized by TIRF microscopy before (left) and after (right) cell lysis. The fluorescence intensity profiles of STAT1-mEGFP in the intact cell and captured on the surface after cell lysis are projected along the yellow lines. The white dashed lines outline the cell shapes prior to lysis. Scale bars: 10 μm.

developed (Supporting Information Figure S2). Efficient NB immobilization and specific capturing of EGFP to NB-functionalized glass surfaces generated by these approaches was confirmed using label-free surface-sensitive detection by reflectance interference spectroscopy[16] (Supporting Information Figure S3). Fluorescence imaging of purified EGFP captured to micropatterned surfaces revealed that a high contrast was achieved by both patterning techniques (Supporting Information Figure S4).

Using these micropatterned surface architectures, we developed single cell pull-down (SiCPull) for probing the stoichiometry and stability of complexes formed by signal transducer and activator of transcription (STAT) proteins, which are latent transcription factors activated by phosphor-

DOI: 10.1021/acs.nanolett.5b01153
Nano Lett. 2015, 15, 3610−3615

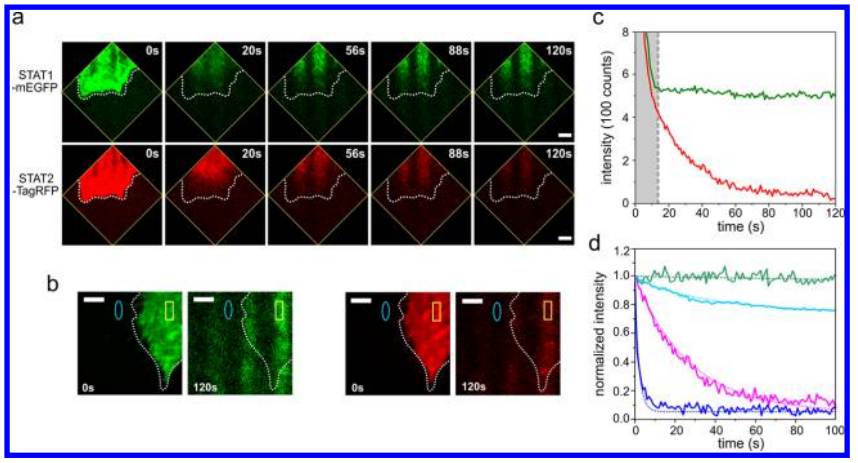

Figure 3. SiCPull assays for determining the dissociation rate constant of different STAT complexes. (a) Time-lapse SiCPull assay after lysis of a HeLa cell coexpressing STAT1-mEGFP and STAT2-TagRFP. Scale bars: 10 μm. (b) The dissociation kinetics was obtained from the fluorescence intensity in the rectangular ROI frame-by-frame corrected for the background signal in the elliptic ROI. Scale bars: 10 μm. (c) Background-corrected fluorescence intensity in the TagRFP channel (red curve) compared to the EGFP channel (green curve). The time regime highlighted in gray corresponds to the time needed for bait protein capturing, which was not considered for kinetic analysis. (d) Comparison of the relative decay in fluorescence intensity upon SiCPull of STAT1-mEGFP coexpressed with different fluorescent-tagged STAT proteins: STAT1 (cyan), STAT2 (magenta), and STAT3 (blue). As a control for photobleaching, pulldown of a mEGFP-TagRFP fusion protein is shown (green). The dissociation rate constants were determined by exponential fits (dotted lines).

ylation via cytokine receptor signaling.[17] Numerous interactions between STATs as well as further effector proteins have been proposed,[18] which have not yet been properly disentangled with respect to affinity, kinetics, and stoichiometry. Here, we focused on STAT1, STAT2, and STAT3, which are tyrosine-phosphorylated upon activation of the type I interferon (IFN) receptor to form homo- and heterodimeric transcription factors.[19,20] These STAT proteins have been reported to form homodimers (STAT1/STAT1)[21,22] and heterodimers (STAT1/STAT2 and STAT1/STAT3)[23] even in the absence of phosphorylation and important regulatory functions of these complexes have been proposed.[24] While the unphosphorylated STAT1/STAT1 homodimer has been in detail characterized in vitro,[22] the existence of unphosphorylated STAT complexes involving STAT2 and STAT3 and their physiological relevance remains debated. Moreover, higher oligomeric states of STAT complexes with even more enigmatic regulatory functions have been proposed.[21,22,25] We here specifically aimed to explore the properties of the postulated STAT1/STAT2 complex, which supposedly plays an important role in the formation of IFN-stimulated gene factor 3 (ISGF3),[26,27] a hallmark transcription factor activated by IFN signaling.

For pull-down of STAT complexes, we employed STAT1 fused to monomeric EGFP (STAT1-mEGFP) as a bait protein. HeLa cells expressing STAT1-mEGFP were cultured overnight on supports presenting the NB in a line-shaped micropattern. The release of cytosolic proteins was initiated by addition of 0.1% Triton X-100, a mild, nonionic detergent, during surface-sensitive imaging by TIRF microscopy (Figure 2 and Supporting Information Video 1). Under these conditions, collapse of the cell and release of the STAT1-mEGFP from the cytosol was observed (Figure 2), while the cell debris including the nucleus remained at the original position. Importantly, STAT1-mEGFP released from the cytosol was efficiently captured to the substrate surface by micropatterned NB covering a region of several ten microns beyond the dimension of the original cell. Thus, efficient capture of bait proteins from single cells was achieved via micropatterned NB.

To probe the proposed interaction of STAT1 and STAT2, HeLa cells transiently expressing STAT1-mEGFP and STAT2 fused to TagRFP (STAT2-TagRFP) were cultured on the micropatterned surface and protein capturing to the surface was monitored by dual color TIRF imaging. Upon cell lysis, STAT1-mEGFP immobilization into micropatterns was observed reaching a constant level after a few seconds (Figure 3a,c and Supporting Information Video 2). Strikingly, binding of STAT2-TagRFP into micropatterns perfectly matching the geometry of EGFP channel was observed, followed by a continuous decay of the signal monitored at a frame rate of 1 Hz over 200 s (Figure 3a). These results suggested efficient capturing of STAT1-mEGFP/STAT2-TagRFP complexes followed by dissociation of STAT2-TagRFP. Control SiCPull experiments with a mEGFP-TagRFP fusion protein confirmed that the decay of the TagRFP signal was not caused by photobleaching (Figure 3d, and Supporting Information Figure S5). Moreover, no surface capturing was observed for cells expressing only TagRFP or STAT2-TagRFP (Supporting Information Figure S6), confirming the high specificity of the pull-down assay. The dissociation of STAT2-TagRFP from the surface was fitted by a monoexponential decay yielding a complex lifetime τ = 24.4 ± 4.7 s for the STAT1-STAT2 complex. The same experiments were carried out with STAT1 and STAT3, respectively, as prey proteins (Supporting Information Figure S7). Efficient pull-down of prey STAT1 was observed as expected for a STAT1/STAT1 homodimer, dissociating substantially slower compared to STAT1/STAT2 complexes (Figure 3d and Supporting Information Figure S7). The lifetime of 41 ± 7.6 min obtained for STAT1/STAT1 complexes was in a good agreement with in vitro data reported previously.[22] Interestingly, we observed a second, faster component of this interaction, which was similar to the STAT1/STAT2 interaction (Table 1) and could be related to a STAT1 homotetramer.[22] In contrast, weaker binding and rapid dissociation of STAT1/STAT3 compared to STAT1/STAT2 complexes was observed, suggesting very low affinity of the STAT1-STAT3 interaction (Figure 3d and Supporting Information Figure S7). These experiments confirmed efficient

DOI: 10.1021/acs.nanolett.5b01153
Nano Lett. 2015, 15, 3610−3615

Table 1. Lifetimes of STAT Complexes Obtained from SiCPull Experiments

prey protein[a]	k_d (s^{-1})	τ^c
STAT1-HaloTag	$(4.0 \pm 0.7) \times 10^{-4}$ $(79.6 \pm 14.7\%)^b$	41 ± 7.6 min
	0.045 ± 0.008 (20.4 ± 3.7%)	22.2 ± 4.1 s
STAT2-TagRFP	0.041 ± 0.008	24.4 ± 4.7 s
STAT3-TagRFP	0.48 ± 0.11	2.1 ± 0.5 s

[a]The bait was STAT1-mEGFP in all cases. [b]Obtained from a biexponential fit, relative amplitudes in brackets. [c]Results are mean ± SD. For complex of STAT2-STAT1, lifetime is obtained from nine different ROIs of three cells, for STAT1-STAT1 and STAT3-STAT1, six ROIs of two cells.

pull-down of functionally relevant transient protein complexes from single cells was possible and dissociation rate constants down to ~0.5 s^{-1} could be quantified by SiCPull, as currently limited by rate of protein release and surface capturing upon cell lysis.

To analyze the stoichiometry of surface-captured complexes by single molecule photobleaching,[28] the density of the NB in the micropatterns was reduced by ~100-fold. Thus, individual protein complexes could be discerned after cell lysis (Figure 4a). For more robust photobleaching analysis, HaloTag-specific posttranslational labeling of the prey protein with tetramethylrhodoamine (TMR) was employed due to higher photostability and less photoblinking of this fluorophore. HeLa cells expressing STAT2-mEGFP and STAT1-HaloTag were labeled with TMR. After cell lysis, substantial colocalization of individual EGFP and TMR signals within micropatterns was observed by single molecule TIRF microscopy (Figure 4a,b). Single molecule colocalization (16% of localized signals colocalized within 100 nm distance), confirmed the formation of STAT1/STAT2 complexes at the single molecule level. The number of STAT1 molecules within individual complexes was determined by analyzing the stepwise fluorescence decay during photobleaching[8,29] (Figure 4c,d and Supporting Information Video 3). While also dissociation of complexes may contribute to the decay, the same information on complex stoichiometry is obtained provided that individual proteins (rather than, e.g., dimers) dissociate. Statistical analysis from >500 individual traces revealed that 74.3% of the localized TMR signals were photobleached within a single step, 24.0% in two steps and 1.7% in multiple steps (Figure 4d). For calibration of the bleaching characteristics for monomeric and dimeric complexes, we performed control experiments with cells expressing mEGFP fused to a single HaloTag (mEGFP-HaloTag) as

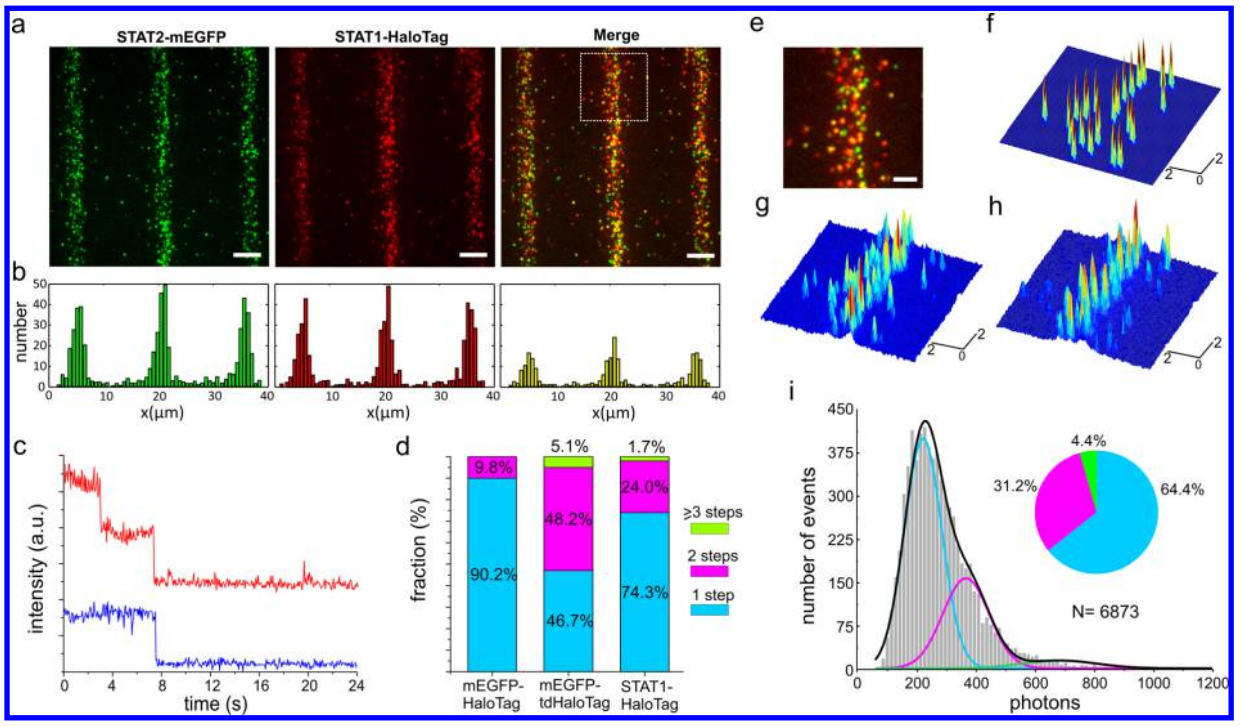

Figure 4. Determination of the stoichiometry of cytosolic complex by SiCPull. (a) Micropatterned STAT2-mEGFP (green channel) and TMR-labeled STAT1-HaloTag (STAT1-^{TMR}HaloTag, red channel) captured in situ from a single HeLa cell as observed immediately after cell lysis. Micropatterned surfaces sparsely functionalized with NB were employed to ensure resolving individual complexes. The overlay of both channels reveals a significant overlap on the single molecule level. Scale bars: 5 μm. (b) Single molecule localization profiles across the micropatterned surface (green channel and red channel) as well as single molecule colocalization within a 100 nm threshold (overlay channel). (c) Typical single molecule photobleaching traces for surface-bound STAT1-^{TMR}HaloTag showing one (blue trace) and two step (red trace) decay. (d) Fraction of events with different numbers of photobleaching steps for determining complex stoichiometries. For comparison, photobleaching step analysis of mEGFP fused to one and two HaloTag proteins, respectively, are shown. More than 500 individual traces for each sample were analyzed. (e–i) Intensity distribution histogram analyses for determining complex stoichiometries. (e) Magnified single molecule SiCPull image in (a) marked by the white square, in which mEGFP (g) and ^{TMR}HaloTag (h) are detected in the corresponding channel, respectively. The colocalized signals within 100 nm distance are picked up in (f). Scale bars: 2 μm. (i) Intensity histogram analysis obtained for STAT1-^{TMR}HaloTag. A three-component Gaussian was used for fitting the histogram (see also Supporting Information Figure S10). Color coding of cyan, magenta, and green marks the intensity fraction of one-, two-, and three-TMR labeled STAT1-HaloTag in the detected complexes, respectively. "N" is the total number of localized signals pooled in the histogram.

DOI: 10.1021/acs.nanolett.5b01153
Nano Lett. 2015, 15, 3610–3615

well as cells expressing mEGFP fused to tandem HaloTag (mEGFP-tdHaloTag) (Supporting Information Figure S8). These calibrations suggest that the majority of STAT1/STAT2 complexes have a 1:1 stoichiometry, while a significant fraction of complexes include two STAT1 molecules, probably due to formation of STAT1/STAT2 heterotetramers. The stoichiometry of STAT1/STAT2 complex was further corroborated by computer-aided step counting analysis[30] (Supporting Information Figure S9) and by single molecule intensity distribution analysis,[31,32] which reliably reproduced the stoichiometries obtained by photobleaching analysis (Figure 4e-i and Supporting Information Figure S10).

In conclusion, we have here established SiCPull as a robust on-chip technique for probing stability and stoichiometry of transient protein complexes on the single cell level. In contrast to previously described single molecule pull-down techniques, which are based on isolation of cell lysates,[8,10−13] cytosolic proteins are captured and analyzed within several seconds after release from the cell. Owing to the rapid association and the high affinity of the NB-GFP complex, highly efficient surface capturing is achieved allowing in situ characterization of protein complexes by ensemble and by single molecule techniques. By using SiCPull, we confirmed formation of homomeric and heteromeric STAT complexes in the absence of receptor stimulation and we could quantitatively map differences in their complex stabilities. Single molecule SiCPull moreover revealed formation of STAT1/STAT2 complexes containing more than one STAT1 molecule. This observation suggests dimerization of STAT1/STAT2 heterodimers, but we currently cannot exclude interactions of STAT1/STAT2 heterodimers with STAT1/STAT1 homodimers. The highly dynamic nature of the STAT1/STAT2 heteromers could explain formation of pSTAT1 homodimers during type I interferon signaling caused by transient docking of STAT1 via STAT2.[26,27]

Versatile binary surface micropatterning allows spatially controlling the organization of capturing groups as well as cell adhesion, thus ensuring simple bottom-up implementation of SiCPull assays. For proof-of-concept experiments, we chose micropatterns providing internal control of capturing specificity. However, more rigid control of cell distribution on the coverslide surface can be achieved by micropatterns providing RGD patches for cell adhesion (Supporting Information Figure S11). By avoiding the preparation of cell lysates, SiCPull allows analyzing complexes from individual cells within heterogeneous populations or cells in different states of activation, which can be microscopically characterized directly before analyzing composition and dynamics of complexes. Combination of micropatterned surface architectures with spatiotemporally controlled lysis of individual cells by means of optical,[33] mechanical,[34] photothermal,[35] or fluidic micromanipulation[36] will enable to pull-down protein complexes one cell at a time.

■ ASSOCIATED CONTENT

Supporting Information

Supplementary figures and tables, detailed materials and methods for surface micropatterning, single cell pulldown experiments, and data evaluation. This material is available free of charge via the Internet at http://pubs.acs.org.

■ AUTHOR INFORMATION

Corresponding Authors

*E-mail: you@biologie.uni-osnabrueck.de.
*E-mail: piehler@uos.de.

Author Contributions

C.Y. and J.P. conceived the project. T.W., S.L., M.B., and C.Y. performed experiments. C.P.R. programmed evaluation software. T.W., C.P.R., J.P., and C.Y. analyzed the data. J.P. and C.Y supervised the project and wrote the manuscript.

Notes

The authors declare no competing financial interest.

■ ACKNOWLEDGMENTS

We thank Gabriele Hikade and Hella Kenneweg for technical support and Rainer Kurre for his support with fluorescence microscopy. This project was supported by the Deutsche Forschungsgemeinschaft (SFB 944).

■ REFERENCES

(1) Grecco, H. E.; Schmick, M.; Bastiaens, P. I. H. *Cell* **2011**, *144* (6), 897−909.
(2) Horvath, C. M. *Trends Biochem. Sci.* **2000**, *25* (10), 496−502.
(3) Brameshuber, M.; Schutz, G. J. *Methods Enzymol.* **2012**, *505*, 159−86.
(4) Piehler, J. *Curr. Opin. Struct. Biol.* **2014**, *24*, 54−62.
(5) Ewing, R. M.; Chu, P.; Elisma, F.; Li, H.; Taylor, P.; Climie, S.; McBroom-Cerajewski, L.; Robinson, M. D.; O'Connor, L.; Li, M.; Taylor, R.; Dharsee, M.; Ho, Y.; Heilbut, A.; Moore, L.; Zhang, S.; Ornatsky, O.; Bukhman, Y. V.; Ethier, M.; Sheng, Y.; Vasilescu, J.; Abu-Farha, M.; Lambert, J. P.; Duewel, H. S.; Stewart, I. I.; Kuehl, B.; Hogue, K.; Colwill, K.; Gladwish, K.; Muskat, B.; Kinach, R.; Adams, S. L.; Moran, M. F.; Morin, G. B.; Topaloglou, T.; Figeys, D. *Mol. Syst. Biol.* **2007**, *3*, 89.
(6) Wepf, A.; Glatter, T.; Schmidt, A.; Aebersold, R.; Gstaiger, M. *Nat. Methods* **2009**, *6* (3), 203−5.
(7) Trinkle-Mulcahy, L. *Proteomics* **2012**, *12* (10), 1623−38.
(8) Jain, A.; Liu, R.; Ramani, B.; Arauz, E.; Ishitsuka, Y.; Ragunathan, K.; Park, J.; Chen, J.; Xiang, Y. K.; Ha, T. *Nature* **2011**, *473* (7348), 484−488.
(9) Jain, A.; Liu, R.; Xiang, Y. K.; Ha, T. *Nat. Protocols* **2012**, *7* (3), 445−452.
(10) Aggarwal, V.; Ha, T. *BioEssays* **2014**, *36* (11), 1109−19.
(11) Jain, A.; Arauz, E.; Aggarwal, V.; Ikon, N.; Chen, J.; Ha, T. *Proc. Natl. Acad. Sci. U.S.A.* **2014**, *111* (50), 17833−8.
(12) Yeom, K. H.; Heo, I.; Lee, J.; Hohng, S.; Kim, V. N.; Joo, C. *EMBO Rep.* **2011**, *12* (7), 690−696.
(13) Lee, H.-W.; Kyung, T.; Yoo, J.; Kim, T.; Chung, C.; Ryu, J. Y.; Lee, H.; Park, K.; Lee, S.; Jones, W. D.; Lim, D.-S.; Hyeon, C.; Do Heo, W.; Yoon, T.-Y. *Nat. Commun.* **2013**, *4*, 1505.
(14) Rothbauer, U.; Zolghadr, K.; Muyldermans, S.; Schepers, A.; Cardoso, M. C.; Leonhardt, H. *Mol. Cell. Proteomics* **2008**, *7* (2), 282−9.
(15) Howorka, S.; Hesse, J. *Soft Matter* **2014**, *10* (7), 931−941.
(16) Schmitt, H. M.; Brecht, A.; Piehler, J.; Gauglitz, G. *Biosens. Bioelectron.* **1997**, *12* (8), 809−816.
(17) Haan, C.; Kreis, S.; Margue, C.; Behrmann, I. *Biochem. Pharmacol.* **2006**, *72* (11), 1538−46.
(18) Chatterjee-Kishore, M.; van den Akker, F.; Stark, G. R. *Trends Cell. Biol.* **2000**, *10* (3), 106−11.
(19) Stark, G. R.; Kerr, I. M.; Williams, B. R.; Silverman, R. H.; Schreiber, R. D. *Annu. Rev. Biochem.* **1998**, *67*, 227−64.
(20) Platanias, L. C.; Fish, E. N. *Exp. Hematol.* **1999**, *27* (11), 1583−92.
(21) Mao, X.; Ren, Z.; Parker, G. N.; Sondermann, H.; Pastorello, M. A.; Wang, W.; McMurray, J. S.; Demeler, B.; Darnell, J. E., Jr.; Chen, X. *Mol. Cell* **2005**, *17* (6), 761−71.
(22) Wenta, N.; Strauss, H.; Meyer, S.; Vinkemeier, U. *Proc. Natl. Acad. Sci. U.S.A.* **2008**, *105* (27), 9238−43.
(23) Stancato, L. F.; David, M.; Carter-Su, C.; Larner, A. C.; Pratt, W. B. *J. Biol. Chem.* **1996**, *271* (8), 4134−4137.
(24) Yang, J.; Stark, G. R. *Cell Res.* **2008**, *18* (4), 443−51.

DOI: 10.1021/acs.nanolett.5b01153
Nano Lett. 2015, 15, 3610−3615

(25) Sehgal, P. B. *Semin. Cell. Dev. Biol.* **2008**, *19* (4), 329−40.
(26) Li, X.; Leung, S.; Kerr, I. M.; Stark, G. R. *Mol. Cell. Biol.* **1997**, *17* (4), 2048−56.
(27) Lochte, S.; Waichman, S.; Beutel, O.; You, C.; Piehler, J. *J. Cell. Biol.* **2014**, *207* (3), 407−18.
(28) Arant, R. J.; Ulbrich, M. H. *ChemPhysChem* **2014**, *15* (4), 600−5.
(29) Ulbrich, M. H.; Isacoff, E. Y. *Nat. Methods* **2007**, *4* (4), 319−321.
(30) Shuang, B.; Cooper, D.; Taylor, J. N.; Kisley, L.; Chen, J.; Wang, W.; Li, C. B.; Komatsuzaki, T.; Landes, C. F. *J. Phys. Chem. Lett.* **2014**, *5* (18), 3157−3161.
(31) Clarke, S.; Pinaud, F.; Beutel, O.; You, C.; Piehler, J.; Dahan, M. *Nano Lett.* **2010**, *10* (6), 2147−2154.
(32) You, C.; Wilmes, S.; Richter, C. P.; Beutel, O.; Lisse, D.; Piehler, J. *ACS Chem. Biol.* **2013**, *8* (2), 320−6.
(33) Heller, I.; Hoekstra, T. P.; King, G. A.; Peterman, E. J. G.; Wuite, G. J. L. *Chem. Rev.* **2014**, *114* (6), 3087−3119.
(34) Raman, A.; Trigueros, S.; Cartagena, A.; Stevenson, A. P. Z.; Susilo, M.; Nauman, E.; Contera, S. A. *Nat. Nanotechnol.* **2011**, *6* (12), 809−814.
(35) Xu, J.; Teslaa, T.; Wu, T.-H.; Chiou, P.-Y.; Teitell, M. A.; Weiss, S. *Nano Lett.* **2012**, *12* (11), 5669−5672.
(36) Hughes, A. J.; Spelke, D. P.; Xu, Z.; Kang, C. C.; Schaffer, D. V.; Herr, A. E. *Nat. Methods* **2014**, *11* (7), 749−55.

DOI: 10.1021/acs.nanolett.5b01153
Nano Lett. 2015, 15, 3610−3615